



HAL
open science

Precision efficiency calibration of a high-purity co-axial germanium detector at low energies

B. Blank, P. Ascher, M. Gerbaux, J. Giovinazzo, S. Grevy, T. Kurtukian Nieto, M. Versteegen, J.C. Thomas

► **To cite this version:**

B. Blank, P. Ascher, M. Gerbaux, J. Giovinazzo, S. Grevy, et al.. Precision efficiency calibration of a high-purity co-axial germanium detector at low energies. Nucl.Instrum.Meth.A, 2020, 984, pp.164631. 10.1016/j.nima.2020.164631 . hal-02557704

HAL Id: hal-02557704

<https://hal.science/hal-02557704>

Submitted on 14 Sep 2022

HAL is a multi-disciplinary open access archive for the deposit and dissemination of scientific research documents, whether they are published or not. The documents may come from teaching and research institutions in France or abroad, or from public or private research centers.

L'archive ouverte pluridisciplinaire **HAL**, est destinée au dépôt et à la diffusion de documents scientifiques de niveau recherche, publiés ou non, émanant des établissements d'enseignement et de recherche français ou étrangers, des laboratoires publics ou privés.



Distributed under a Creative Commons Attribution - NonCommercial 4.0 International License

Precision efficiency calibration of a high-purity co-axial germanium detector at low energies

B. Blank^{1, a}, P. Ascher, ^a M. Gerbaux, ^a J. Giovinazzo, ^a S. Grévy, ^a T. Kurtukian Nieto, ^a
M. Versteegen, ^a J.C. Thomas ^b

^aCentre d'Etudes Nucléaires de Bordeaux Gradignan - UMR 5797, CNRS/IN2P3 - Université de Bordeaux, 19, Chemin du Solarium, CS 10120, F-33175 Gradignan Cedex, France

^bGrand Accélérateur National d'Ions Lourds, CEA/DRF - CNRS/IN2P3, Bud Henri Becquerel, BP 55027, F-14076 CAEN Cedex 5, France

Abstract

Following work done in the energy region above 100 keV, the high-precision calibration of a co-axial high-purity germanium detector has been continued in the energy region below 100 keV. Some of the previous measurements and Monte-Carlo simulations have been repeated with higher statistics and a new source measurement with ¹⁶⁹Yb has been added. For the energy range from 40 keV to 100 keV, an absolute precision for the detection efficiency of $\pm 0.2\%$ has been reached, as previously obtained for energies above 100 keV. The low-energy behaviour of the germanium detector was further scrutinized by studying the germanium X-ray escape probability for the detection of low-energy photons. In addition, one experimental point, a γ ray at 2168 keV from the decay of ³⁸K, has been included for the total-to-peak ratios agreeing well with simulations. The same γ ray was also added for the single- and double-escape probabilities. Finally, the long term stability of the efficiency of the germanium detector was investigated by regularly measuring the full-energy peak efficiency with a precisely calibrated ⁶⁰Co source and found to be perfectly stable over a period of 10 years.

Key words: gamma-ray spectroscopy, germanium detector, Monte-Carlo simulations

PACS: 07.85.-m, 29.30.Kv, 23.20.-g

1. Introduction

Gamma-ray spectroscopy is a powerful tool for the study of nuclear structure. In particular, β -decay studies are often performed by measuring γ -ray intensities to deduce β -decay feeding probabilities. This applies in particular to high-precision β -decay measurements as conducted for the purpose of weak-interaction studies. To determine the value of super-allowed β decays of the $0^+ \rightarrow 0^+$ type, high-precision measurements are required for the Q_{EC} value, the half-life, and the super-allowed branching ratio. The latter quantity is usually determined by measurements of the γ -decay probabilities of excited levels in the β -decay daughter nucleus, from which the β -decay feeding probabilities are determined.

Our group has a long standing experimental program of measuring half-life values and branching ratios of these super-allowed β decays [1–8] or of mirror decays [6,9,10], where high-precision γ -ray spectroscopy is required. There-

fore, we have started in 2010 to precisely calibrate a high-purity (HP), n-type, co-axial germanium detector with a relative efficiency of 70%. The germanium crystal has an active volume of 278 cm³ corresponding to about 1.48 kg of germanium. The most important part of this calibration work was published a few years ago [11]. In recent years, we continued this calibration work, in particular to improve the precision below 100 keV γ -ray energy, where we gave an absolute precision of only $\pm 0.5\%$ in our previous work. This was mainly due to the fact that, at low energies, many background γ rays "pollute" the spectrum and we had not enough information to ascertain that we achieved the same precision as above 100 keV.

For a measurement recently performed with ²²Mg, we need precise efficiencies in the energy range below 100 keV, which was the prime reason to extend the high-precision efficiency calibration of our detector down to 40 keV. In the present work, we describe measurements with a new source (¹⁶⁹Yb). In addition, new measurements were performed with higher statistics as compared to our previous work with sources already used there (²⁴Na, ⁴⁸Cr and

¹ Corresponding author: B. Blank, blank@cenbg.in2p3.fr

40 ^{207}Bi). Higher-statistics Monte-Carlo (MC) simulations
 41 have been performed for ^{133}Ba , ^{152}Eu and $^{180}\text{Hf}^m$. The
 42 new experimental data for ^{24}Na , ^{48}Cr , and ^{169}Yb were
 43 taken at ISOLDE, whereas the ^{207}Bi data come from a
 44 source measurement.

Table 1
 ^{169}Yb and $^{180}\text{Hf}^m$ source characteristics used to determine the de-
 tector efficiency. The characteristics of the other sources are given
 in [11].

Nuclide	$T_{1/2}$	E_γ (keV)	P_γ	Reference
^{169}Yb	32.016 d	50.4	1.464(21)	[12]
		58.0	0.3855(81)	
		63.1	0.4405(24)	
		93.6	0.02571(17)	
		109.8	0.1736(9)	
		118.2	0.01870(10)	
		130.5	0.1138(5)	
		177.2	0.2232(10)	
		198.0	0.3593(12)	
$^{180}\text{Hf}^m$	5.53 h	307.7	0.10046(45)	
		57.5	0.4799(94)	[13]
		93.3	0.1751(14)	[14]
		215.3	0.8150(15)	[14]
		332.3	0.9443(05)	[14]
		443.1	0.8180(130)	[14]
		500.7	0.1421(28)	[13]

45 We took also data at ISOLDE for ^{49}Cr , which, according
 46 to literature, should have had well determined branching
 47 ratios for γ rays between 62 keV and 153 keV, ideal to
 48 connect the region above 100 keV already well calibrated in 70
 49 our previous work and the region below 100 keV. However, 71
 50 it turned out that the branching ratios were not at all in
 51 agreement with the γ -ray rates we observed. Therefore, 72
 52 instead of using ^{49}Cr to calibrate our detector, we used 73
 53 this latter to propose a new measurement of the branching 74
 54 ratios of this isotope [15]. 75

55 The general outcome of the present work is that the de- 76
 56 tector model developed in our previous work is also valid 77
 57 with the same precision below 100 keV. Only for data points 78
 58 below 40 keV we seem to start having systematic discrep- 79
 59 ancies between experimental data and simulations. It is not 80
 60 clear whether this is a problem with our detector model 81
 61 or rather linked to electronics issues with the trigger effi- 82
 62 ciency. We refrain from speculating about the reason for 83
 63 this discrepancy and assume that the efficiency of our de- 84
 64 tector is precise at a level of $\pm 0.2\%$ down to a γ -ray energy 85
 65 of 40 keV. 86

66 The detector model used for the simulations in the 87
 67 present work is the same as in [11]. It is shown in fig- 88
 68 ure 1. The main characteristics of the detector are given in 89
 69 table 2. 90

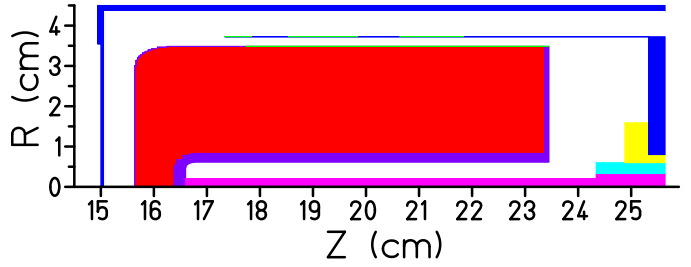


Fig. 1. Detector model as used in CYLTRAN or GEANT4 simu-
 lations. The colour code is as follows: red: germanium; violet: germa-
 nium dead material; blue: aluminum; pink: brass. The upper green
 material (difficult to see, on the top of the germanium material)
 corresponds to screws from the detector holding structure, which,
 in CYLTRAN, had to be "distributed" over a hollow cylinder. The
 other colours correspond to isolating material and teflon. The source
 sits for all measurements at the origin of the coordinate system.

Table 2
 Detector characteristics used in the modelling of the germanium
 detector.

	parameters
length of crystal	78.10 mm
radius of crystal	34.84 mm
length of central hole	68.5 mm
radius of central hole	6.1 mm
external dead zone	8.5 μm
internal dead zone	2.2 mm
back-side dead zone	0.8 mm
distance window - crystal	5.7 mm
entrance window thickness	0.7 mm

2. Experimental results with γ -ray sources and comparison with CYLTRAN simulations

In the present work, we have adopted the branching ratios for $^{180}\text{Hf}^m$ proposed by Helmer *et al.* [14] and from ENSDF [13] in our analysis and in the decay scheme simulations, because we found them in much better agreement with our data than those used previously [11]. The branching ratios used in the present work for ^{169}Yb and $^{180}\text{Hf}^m$ are given in Table 1. All other source characteristics are the same as presented in our previous paper. The commercial sources had activities on thin mylar foils such that the mylar itself had no influence on the γ -ray flux, even at very low energies. The sources produced on-line at ISOLDE were deposited with an energy of 30 keV at the surface of a small plastic cylinder (diameter 2 cm, thickness 5 mm). The high-energy γ -ray sources ^{56}Co and ^{66}Ga were produced by irradiating enriched ^{56}Fe (56 μm thick) and ^{nat}Zn (5 μm) targets with protons. All source measurements were performed under identical condition on a measurement set-up with a source holder positioning the activities at exactly 15.000(5) cm from the entrance window of the germanium

91 detector.

92 As in our previous work [11], we obtained relative effi-146
 93 ciencies for each γ -ray peak of each source by determining47
 94 the number of counts in each photopeak and deviding this48
 95 number by the branching ratio of the peak, the measure-149
 96 ment time, and the dead time. The latter two can in prin-150
 97 ciple be neglected, as these numbers are the same for all151
 98 γ -ray peaks of a given source. The source activity is a free
 99 parameter that allows to match the experimental data and
 100 the MC simulations. Once the activity adjustment is done,
 101 the difference of the individual experimental and MC effi-
 102 ciencies normalised by the experimental efficiencies is de-
 103 termined. This quantity is a measure for the agreement be-
 104 tween experimental data and MC simulations and is plot-
 105 ted in figure 2 together with the absolute experimental ef-
 106 ficiencies as a function of the γ -ray energies.

107 The main errors come from the fit of the photopeaks and
 108 the uncertainties with which the branching ratios of the
 109 different sources are known. The peak integrals are deter-
 110 mined by a fit with a Gaussian plus a low-energy tail to take
 111 incomplete charge collection into account and a background
 112 function. This fit yields the number of counts in the peak
 113 and its statistical uncertainty. To determine a systematic
 114 uncertainty, we use three different background functions: i)
 115 a second-order polynominal, ii) a linear step function (com-
 116 plement of an error function and a straight line), and (iii)
 117 two independent linear functions left and right of the peak
 118 "smoothly" connected under the peak. We chose for each152
 119 peak to be fit the two most appropriate background func-153
 120 tions. The fit with the best χ^2 is the reference fit, whereas154
 121 we use the second best fit to determine a systematic un-155
 122 certainty from the different integrals of the two fits. More156
 123 details can be found in our previous work [11]. 157

124 Part a) of figure 2 gives the absolute efficiency as a158
 125 function of energy established with 15 different radioactive159
 126 sources, standard sources commercially available, but also160
 127 short-lived sources we produced at ISOLDE or IJCLab Or-161
 128 say. In part b), we give the residuals between the experi-162
 129 mental data and the MC simulations with the CYLTRAN163
 130 code [16]. The vast majority of data lies within $\pm 2\%$. The164
 131 residuals are consistent with no difference between the mea-165
 132 surements and the simulations, which is expected as the166
 133 absolute normalisation is a free parameter for all sources167
 134 except for the ^{60}Co source the activity of which has a pre-168
 135 cision of 0.09%. To verify that the detection efficiency is169
 136 correctly described by our detector model, one has to in-170
 137 spect the residuals for a given source and check that there171
 138 is a zero difference between experimental and simulation172
 139 data for low- and high-energy data points. 173

140 2.1. Detection efficiency below 100 keV

141 A fine analysis of the residuals can give more insights178
 142 about the precision of our detector model in different re-179
 143 gions of energy. As a first step, we present in part c) and d)180
 144 of figure 2 the residuals for γ -ray energies below and above181

500 keV, respectively. The data are the same as in part
 b) of the figure, in particular no change in normalisation
 was operated, whereas the fit is performed only on the re-
 spective parts of the data. As indicated in the figures, the
 residuals are in agreement with no difference between exper-
 iment and simulations. For the three residual plots, the
 χ^2_ν is close to unity.

Table 3

Averages of residuals between the experimental efficiency and the
 simulated ones. For the present table we analysed different regions of
 energies and calculated weighted averages of the individual residuals.

Energy range	average residuals (%)
30 - 500 keV	-0.031(099)
30 - 400 keV	-0.030(100)
30 - 300 keV	-0.188(125)
30 - 200 keV	-0.216(140)
30 - 100 keV	-0.401(288)
30 - 60 keV	-0.593(462)
40 - 500 keV	0.003(100)
40 - 400 keV	-0.001(101)
40 - 300 keV	-0.148(127)
40 - 200 keV	-0.166(144)
40 - 100 keV	-0.197(316)
40 - 60 keV	+0.032(614)

A more refined analysis is presented in table 3 for the
 low-energy part of our measurements. We selected differ-
 ent ranges of energies and determined whether or not the
 averages of the residuals are still in agreement with zero or
 not. Due to the energy selection, this analysis includes only
 part of the γ rays for the different sources. No change of
 the normalisation of source activities was made. If a devi-
 ation from zero is found, this means that for one or several
 sources less agreement is found e.g. for low energies.

This is the case for energies below 40 keV. Although the
 error bars increase significantly when using less and less
 data, there seems to be a general tendency of more and more
 negative average residuals for the low-energy part. This indi-
 cates that there is missing experimental decay strength,
 which could come from a problem with the trigger proba-
 bility for these low γ -ray energies. Another possible expla-
 nation could be that the detector model we use is wrong
 with e.g. the detector entrance window or the detector dead
 layer being too thin. However, in order to match experi-
 ment and simulation, we would need to increase the window
 thickness by more than 50%, which is in contradiction with
 other measurements e.g. with an electron beam [11]. The
 dead layer would need to be increased by an even higher
 factor.

Therefore, we decided to limit our conclusions to energies
 larger than 40 keV. Above this energy we have very good
 agreement between model calculations and experiment. As
 we do not find any difference in agreement between the low-
 energy part (40 - 100 keV) and the high-energy part treated
 in reference [11], we conclude that the absolute precision on

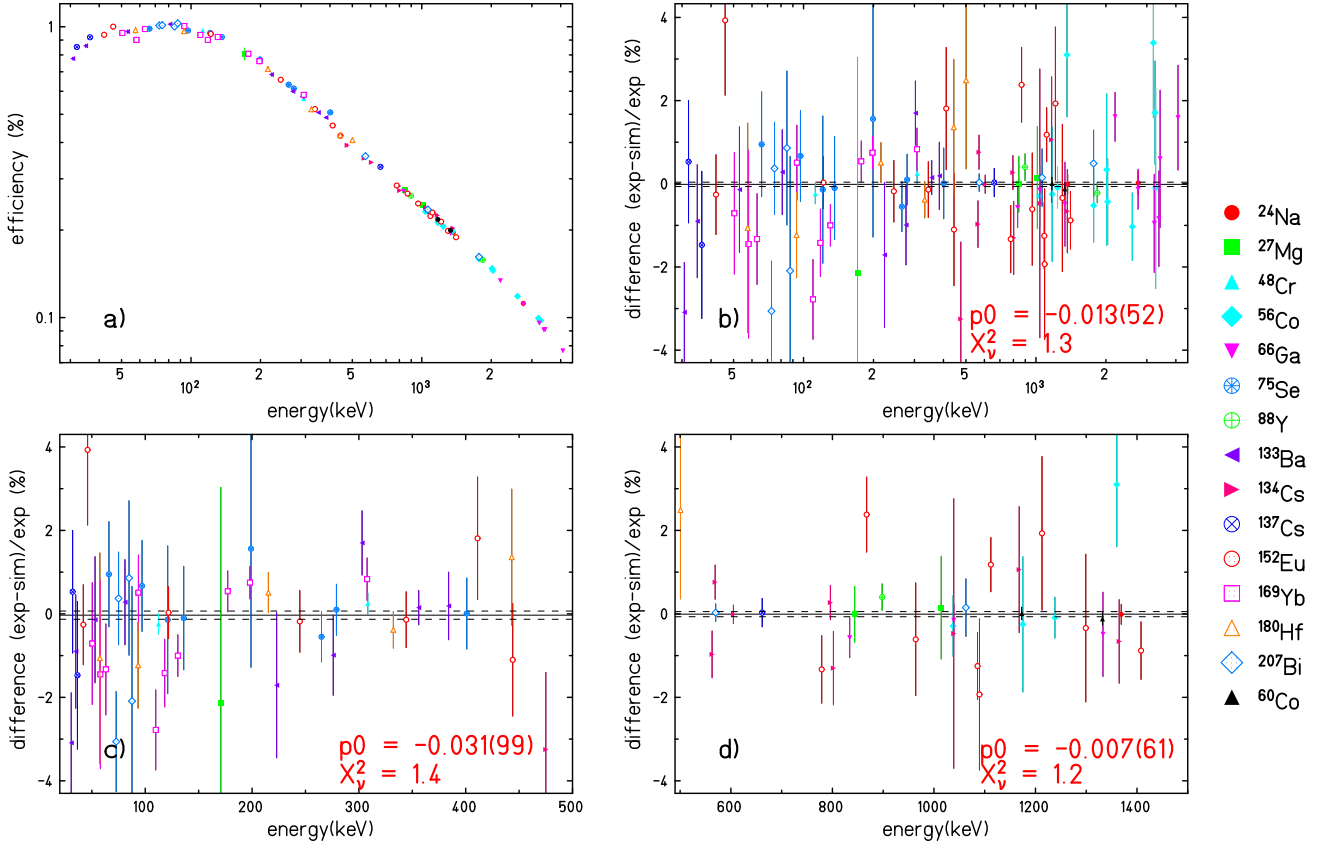


Fig. 2. Full-energy efficiencies and residuals for the γ -ray detection efficiency for all multi- γ -ray sources measured with the present detector. Compared to our previous publication [11], higher-statistics measurements have been performed for the ^{24}Na , ^{48}Cr and ^{207}Bi sources. As an additional source, ^{169}Yb has been added for its low-energy γ rays. Part a) shows the absolute efficiency of the germanium detector over the full range of 30 keV to 4 MeV. Part b) gives the residuals with respect to the MC calculations with the CYLTRAN code over the same energy range. In part c), we zoom on the energy range from 30 keV to 500 keV, whereas part d) shows the residuals in the region from 500 keV to 1500 keV. The fit for this latter figure was made over the range 500 keV - 4000 keV. See text for details.

182 the efficiency of the germanium detector is $\pm 0.2\%$ over the
 183 energy range of 40 keV to 4 MeV, with a relative efficiency
 184 precision of $\pm 0.15\%$ over this energy range.

185 2.2. Total-to-peak ratio as well as single- and 186 double-escape ratios

187 As lead out in our previous work, the ideal source to
 188 determine total-to-peak ratios is an isotope with a single γ
 189 ray and no other decay radiation. ^{38}K comes close to that.
 190 It decays with a half-life of 7.65 min to basically a single
 191 level at 2167 keV (branching ratio of 99.8%) in ^{38}Ar , which
 192 subsequently emits a γ ray of this energy.

193 In figure 3, we have updated the total-to-peak ratio plot
 194 for our detector by including this data point for ^{38}K taken
 195 at ISOLDE. This additional data point is of interest, as it is
 196 much higher in energy than the other data used up to now.
 197 The new experimental data point is in good agreement with
 198 our detector model and confirms that matter around the
 199 detector has to be added to correctly describe the total-to-
 200 peak ratios in our MC simulations (see [11] for details). 202

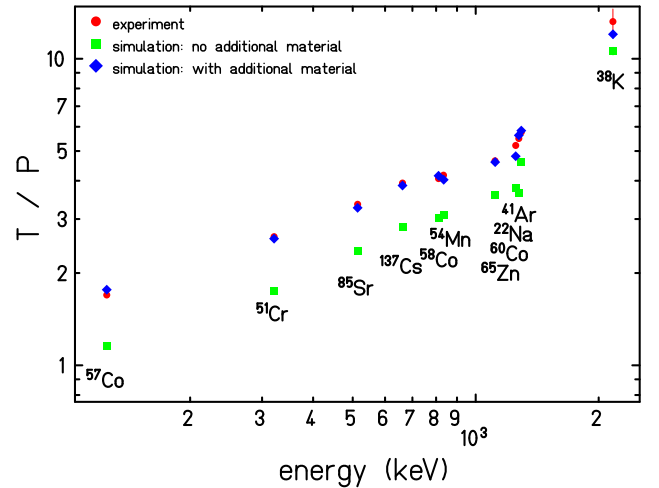


Fig. 3. Total-to-Peak ratio for γ -ray energies ranging from 122 keV to 2170 keV. The good agreement between experiment and simulation already obtained up to 1300 keV in our previous work is extended to 2170 keV.

In a similar way, we also included the ^{38}K data point in the plot of the single-escape and double-escape probabili-

ties for the 511 keV annihilation radiation (figure 4). Good agreement is achieved between experiment and MC simulations.

mined one. No scaling factor is needed. We conclude therefore that, for our detector, CYLTRAN treats correctly this X-ray escape probability.

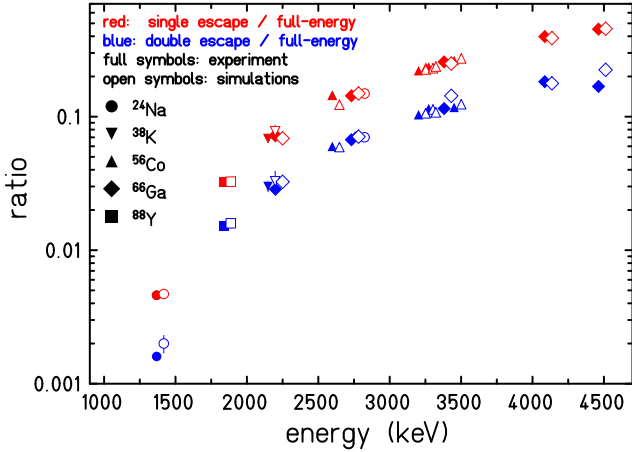


Fig. 4. Ratios of the single-escape (red) and double-escape (blue) intensities over the full-energy intensities from source measurements with ^{24}Na , ^{38}K , ^{56}Co , ^{66}Ga , and ^{88}Y . Full symbols represent experimental ratios, open symbols, slightly shifted to facilitate the reading of the figure, are from simulations with the CYLTRAN code. The additional point for ^{38}K fits nicely in the systematics.

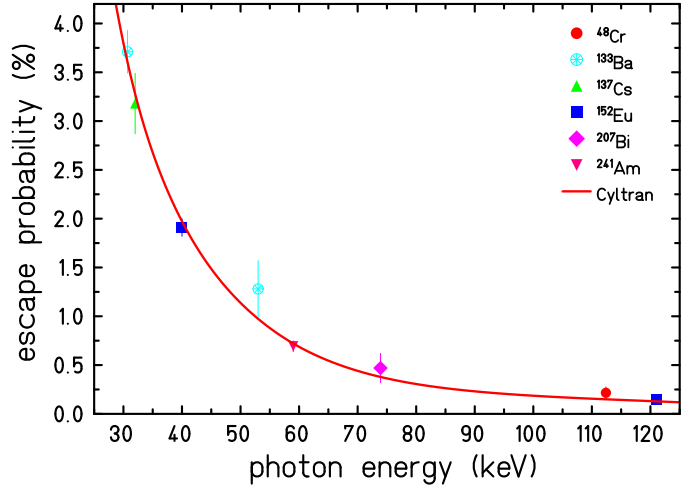


Fig. 5. X-ray escape probability for low-energy photons as measured with the germanium detector and simulated with the CYLTRAN code. The symbols give the experimental data points, whereas the full line stems from CYLTRAN simulations.

3. X-ray escape probability for low-energy photon detection

An effect, which becomes important for photon energies below 100 keV, is the possibility of germanium X-ray escape. At low energies, the interaction of a photon takes place at the very entrance of the germanium crystal. When the photon interacts by photo-electric effect or by Compton scattering, vacancies are created in the electronic shells of the germanium atoms, which are filled by electrons from higher-lying shells thus creating X-rays. These X-rays are of low energy (of order 10 keV) and are usually absorbed by the germanium crystal. However, the closer the interaction occurs to the surface of the germanium crystal (i.e. the lower the photon energy), the higher is the probability of the X-rays to escape from the detector thus creating an event with less energy. Therefore, for low-energy X-ray or γ -ray peaks, a small satellite peak about 10 keV below the main peak can be observed, the intensity of which increases with decreasing energy.

Helmer and co-workers [14] found that their MC simulations underestimate this effect by a factor of 1.16. After scaling the escape probability by this factor, they found satisfying agreement between simulations and experimental measurements. The authors argued that the assumption of a uniform detector surface as well as of complete charge collection in the surface area might be questionable.

As we demonstrate in figure 5, we find agreement over the full energy range from 30 keV to 120 keV between the simulated escape probability and the experimentally deter-

4. Long-term stability of the absolute efficiency with ^{60}Co sources

Our germanium detector is kept cold all year long since more than 10 years (except e.g. for travel to experimental sites in Jyväskylä or at ISOLDE). The reason for that is to avoid that the lithium used for the p contacts diffuses in or out of the detector and thus changes the efficiency of the detector.

In order to verify the efficiency of our detector, we performed several measurements over the years with a ^{60}Co source, which is calibrated in activity with a precision of better than 0.1%. Data were last taken with this source at the end of 2019. As ^{60}Co has a half-life of 5.271 y, the activity has now decreased too much to still use this original source.

We have therefore calibrated a new ^{60}Co source with a precision of 0.14%, which will be used in the future. This source has the same mounting as the old source. The calibration was performed with respect to the old precision source in several runs during 2018. A first verification of the detector efficiency was performed with the new source beginning of 2020 yielding agreement with the initial efficiency (see figure 6).

All efficiency values determined over the last 10 years are in agreement with each other and with the CYLTRAN simulations used as a reference. The numerical values of the efficiencies determined for the two γ rays of ^{60}Co are given in table 4. We can thus conclude that, when keeping the detector cold, a germanium detector can have an efficiency stable over periods of 10 years and more.

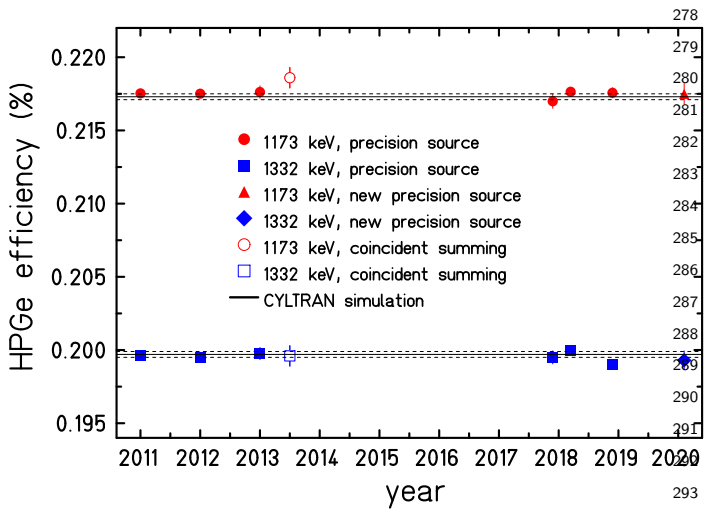


Fig. 6. Long-term stability of the absolute detection efficiency of the germanium detector. The efficiency is stable over a period of 10 years. The last data point has been measured with a new ^{60}Co source calibrated with respect to our old source in August-October 2018 by means of the germanium detector presently described. This source, with an activity of 19.948(28) kBq on August 2, 2018, has a precision on its activity ($\Delta A/A = 0.14\%$) slightly worse than our previous source ($\Delta A/A = 0.09\%$). The precision of the last data point in the plot is limited by the detection statistics. The full lines represent the calculated efficiencies from the CYLTRAN code with the dashed lines being the error bars.

Table 4
Efficiency values as determined in different measurements over the last 10 years for the two γ rays from ^{60}Co . The data taking in 2014 corresponds to a measurement where the method of coincident summing with a strong ^{60}Co source of unknown activity was used (see [11]). The 2020 measurement was performed with a new source calibrated with respect to our old high-precision ^{60}Co source (see text).

year	$\epsilon(1173 \text{ keV})$ (%)	$\epsilon(1332 \text{ keV})$ (%)
2011	0.21753(18)	0.19966(13)
2012	0.21751(19)	0.19949(16)
2013	0.21763(42)	0.19976(42)
2014	0.21860(70)	0.19960(70)
2018	0.21699(48)	0.19950(44)
2018	0.21764(31)	0.19998(29)
2019	0.21757(34)	0.19901(35)
2020	0.21750(70)	0.19930(64)

5. Conclusions

We have continued the efficiency calibration of a germanium detector for high-precision γ -ray spectroscopy. This detector is used primarily for branching-ratio measurements of super-allowed $0^+ \rightarrow 0^+$ decays where precisions of the branching ratios of the order of 0.2% or better are needed. With the present study, we achieved a precision of the absolute detection efficiency for energies down to 40 keV of 0.2% and of the relative detection efficiency of 0.15%.

During recent years, we had access to short-lived sources produced at ISOLDE, which we used to add in particular measurements below 100 keV. We thus added ^{169}Yb as a new source, which has well-known γ rays between 50 keV and 300 keV. In addition, we improved previous measurements by increasing the detection statistics or by increasing the statistics of our MC simulations.

Measurements and simulations of the X-ray escape probability as a function of photon energy allowed us to further confirm the good understanding of the low-energy response of our detector.

Finally, we added a high-energy source, ^{38}K . This isotope has a single high-energy γ ray which allowed us to verify the total-to-peak ratio above 2 MeV. This source also yielded an additional data point for the single- and double-escape probability for annihilation radiation.

Acknowledgment

We thank K. Johnston and U. Köster for their help during the sample collection at ISOLDE.

References

- [1] B. Blank *et al.*, Phys. Rev. C **69**, 015502 (2004).
- [2] G. Canchel *et al.*, Eur. Phys. J. A **29**, 409 (2005).
- [3] A. Bey *et al.*, Eur. Phys. J. A **36**, 121 (2008).
- [4] I. Matea *et al.*, Eur. Phys. J. A **37**, 151 (2008).
- [5] T. Kurtukian Nieto *et al.*, Phys. Rev. C **80**, 035502 (2009).
- [6] B. Blank *et al.*, Eur. Phys. J. A **44**, 363 (2010).
- [7] J. Souin *et al.*, Eur. Phys. J. A **47**, 40 (2011).
- [8] B. Blank *et al.*, Eur. Phys. J. A **51**, 8 (2014).
- [9] A. Bacquias *et al.*, Eur. Phys. J. A **48**, 155 (2011).
- [10] C. Magron *et al.*, Eur. Phys. J. A **53**, 77 (2017).
- [11] B. Blank *et al.*, Nucl. Instr. Meth. A **776**, 34 (2015).
- [12] IAEA STI/PUB/1287-VOL1 (2007).
- [13] <http://www.nndc.bnl.gov/ensdf/>.
- [14] R. G. Helmer *et al.*, Nucl. Instr. Meth. A **511**, 360 (2003).
- [15] B. Blank *et al.*, Eur. Phys. J. A **54**, 93 (2018).
- [16] J. A. Halbleib and T. A. Mehlhorn, Nucl. Sci. Eng. **92**, 338 (1986).